Proceedings of the 42nd IEEE
Conference on Decision and Control
Maui, Hawaii USA, December 2003

Decentralized Control of Autonomous Vehicles[1]

John S. Baras, Xiaobo Tan, and Pedram Hovareshti
Institute for Systems Research and
Department of Electrical and Computer Engineering
University of Maryland, College Park, MD 20742 USA
{baras, xbtan, hovaresp}@glue.umd.edu

Abstract

Decentralized control methods are appealing in coordination of multiple vehicles due to their low demand for long-range communication and their robustness to single-point failures. In this paper we explore a decentralized approach to path generation for a group of vehicles in a battlefield scenario. The mission is to maneuver the vehicles to cover a target area while avoiding obstacles and threats during the maneuver. Each vehicle makes its moving decision by minimizing a potential function that encodes information about its neighbours, obstacles, threats and the target. Preliminary analysis of vehicle behaviors is conducted. Simulation has shown that this approach leads to interesting emergent behaviors, and the behaviors can be varied by adjusting the weighting coefficients of different potential function terms.

1 Introduction

Autonomous unmanned vehicles (AUVs) have potentially revolutionizing applications in defense, transportation, weather forecast, and planetary exploration [1]. These vehicles can be deployed in groups to perform complicated missions. Communication is often limited in these applications due to the large number of vehicles involved, limited battery power, and constraints imposed by environmental conditions or mission requirements. Hence a decentralized approach to coordination and control of multi-vehicles is especially appealing. Another advantage of decentralized methods over centralized ones is their robustness to single-point failures.

Inspired by the emergent behaviors demonstrated by swarms of bacteria, insects, and animals, control methods that yield desired collective behaviors based on simple local interactions have received great interest [2, 3, 4, 5, 6]. Artificial potentials or digital pheromones are often involved in such methods for multi-vehicle control, see e.g., [3, 7, 8, 4] and the references therein. The potential function method has been used in various robotic applications [9], where the force or other input (e.g., the velocity) is derived from some potential function that encodes relevant information about the environment and the mission.

In this paper we explore a decentralized approach to path generation for a group of vehicles in a battlefield scenario using the potential function method. The mission is to maneuver the vehicles to cover a target area while avoiding obstacles and threats. At every time instant each vehicle evaluates its potential function profile and decides its velocity using the gradient descent method. The potential function consists of several terms reflecting the objective and the constraints. It is constructed in such a way that only information about neighbouring vehicles, local information about dynamic threats, and some static information (about stationary threats, targets) are involved. Some qualitative behaviors of the vehicles are discussed. In particular, the behavior of a vehicle experiencing both attraction from the target and repulsion from the obstacles is studied through the vector field analysis. Simulation results have shown that the decentralized approach leads to interesting emergent behaviors, and the behaviors can be varied by adjusting the weighting coefficients of diffrent potential function terms.

The remainder of the paper is organized as follows. In Section 2 the problem setup is described and the potential functions constructed. Analysis of vehicle behaviors is performed in Section 3. Simulation results are reported in Section 4. Section 5 concludes the paper.

2 Potential Functions

We study the kinematic planning problem for N vehicles moving on a (two dimensional) plane. Extension to three dimensional space is straightforward, although the analysis will be more complicated. The task for the vehicles is to move toward and then occupy a connected target area $A \subset \mathbb{R}^2$. They should avoid to crash into

[1]This research was supported by the Army Research Office under the ODDR&E MURI01 Program Grant No. DAAD19-01-1-0465 to the Center for Networked Communicating Control Systems (through Boston University), and under ARO Grant No. DAAD190210319.

obstacles that are distributed in the battlefield. There are also threats, both stationary ones and moving ones, that endanger the vehicles if they are close. It is assumed that each vehicle has the knowledge of locations of stationary threats. A vehicle detects a moving threat if the threat is within the distance R_d, and is destroyed by the threat if the distance between them is less than R_e ($< R_d$). The vehicles can communicate with each other and exchange information about their positions if they are within the neighbouring distance R_c. There is a desired inter-vehicle distance r_0 (less than R_c) for several reasons: staying too close leads to small area of coverage, good chance of collision, and easy targeting by the enemy fire, while staying too far apart leads to loss of communication and coordination.

We order the vehicles and identify each vehicle with its index. Each vehicle is treated as a point. Denote the position of the vehicle i at time t as $p_i(t) = (x_i(t), y_i(t))$. Let $\mathcal{V}(t)$ be the set of vehicles that are alive at t, and $\mathcal{N}_i(t)$ be the neighbouring set of the vehicle i defined by $\mathcal{N}_i(t) \triangleq \{j \in \mathcal{V}(t) : j \neq i, \|p_i(t) - p_j(t)\| \leq R_c\}$. From the previous discussions, there are multiple objectives/constraints when a vehicle makes the moving decision. To accomodate this a potential function is constructed for each vehicle that consists of several terms, each term reflecting a goal or a constraint. To be specific, the potential function $J_{i,t}(p_i)$ for the vehicle i at t is expressed as

$$J_{i,t}(p_i) = \lambda_g J^g(p_i(t)) + \lambda_n J^n_{i,t}(p_i(t)) + \lambda_o J^o(p_i(t)) + \lambda_s J^s(p_i(t)) + \lambda_m J^m_t(p_i(t)), \quad (1)$$

where $J^g, J^n_{i,t}, J^o, J^s, J^m_t$ are the components of the potential function relating to the target, neighbouring vehicles, obstacles, stationary threats, and moving threats, respectively, and $\lambda_g, \lambda_n, \lambda_o, \lambda_s, \lambda_m \geq 0$ are the corresponding weighting coefficients. The velocity $\dot{p}_i$ is then given by

$$\dot{p}_i(t) = -\frac{\partial J_{i,t}(p_i)}{\partial p_i}. \quad (2)$$

We now describe in detail the components of $J_{i,t}$:

(1) The target potential J^g. $J^g(p_i) = f_g(\rho(p_i, A))$, where $\rho(p_i, A) = \inf_{a \in A} \|p_i - a\|$ (the distance from p_i to the target area A), $f_g(\cdot)$ is a strictly increasing function, and $f_g(0) = 0$. This guarantees that in the absence of other objects, the vehicle will move toward the target. For analysis and simulation in this paper, we choose $f_g(r) = r^2$;

(2) The neighbouring potential $J^n_{i,t}$.

$$J^n_{i,t}(p_i) = \sum_{j \in \mathcal{N}_i(t)} f_n(\|p_i - p_j(t)\|),$$

where $f_n : \mathbb{R}^+ \to \mathbb{R}$ is a differentiable function that has the following properties: a) $f_n(r)$ approaches infinity as $r \to 0$, and is strictly decreasing on $[0, r_0]$; b) it is strictly increasing on $[r_0, R_c]$ and $\frac{df_n}{dr} = 0$ on $[R_c, \infty)$. These properties enable two vehicles to keep the optimal distance in the absence of other objects, and make the transition of dynamics seamless when the neighbouring set of a vehicle is changing. An appropriate combination of $\frac{1}{r^2}$, $(r - r_0)^2$, and $-(r - R_c)^2$ is used for f_n in our simulation;

(3) The obstacle potential J^o. An obstacle is a connected, closed set (could be a single point) that a vehicle cannot enter. Assume that there are a finite number of obstacles $\{O_j\}_{j=1}^{N_o}$. Let $J^o(p_i) = \sum_{j=1}^{N_o} f_o(\rho(p_i, O_j))$, where $\rho(p_i, O_j)$ is the distance from p_i to the set O_j, and $f_o(\cdot) : \mathbb{R}^+ \to \mathbb{R}$ is a strictly decreasing function that satisfies $f_o(r) \to \infty$ as $r \to 0$. In this paper f_o is chosen to be $\frac{1}{r^2}$. The information about obstacles can be obtained beforehand, or it can be available "on the fly" through detection;

(4) The potential J^s due to stationary threats. Stationary threats can be modeled similarly as obstacles, so that vehicles will tend to stay away from them. Anisotropic (direction-dependent) threats can also be included using appropriate potential functions;

(5) The potential J^m_t due to moving threats. A moving threat is modeled as a moving point. Let $\mathcal{M}_i(t)$ be the set of moving threats that are within the detection range of the vehicle i, and q_j be the position of the threat j. Let $J^m_t(p_i) = \sum_{j \in \mathcal{M}_i(t)} f_m(\|p_i - q_j\|)$, where the function $f_m : (R_e, \infty) \to \mathbb{R}$ is differentiable, strictly decreasing on (R_e, R_d), constant on (R_d, ∞), and $f_m(r) \to \infty$ when $r \to R_e$. With this potential function, a vehicle tends to keep at least a distance R_e from moving threats, and its vector field remains continuous when moving threats enter or leave its detection range. A simple example for such $f_m(\cdot)$ is

$$f_m(r) = \begin{cases} \frac{1}{(r-R_e)^2} & \text{if } R_e < r \leq \frac{a_2}{2} \\ \frac{16(r-R_d)^2}{a_1^3 a_2} - \frac{8R_e}{a_1^3} & \text{if } \frac{a_2}{2} \leq r \leq R_d \\ -\frac{8R_e}{a_1^3} & \text{if } r > R_d \end{cases},$$

where $a_1 \triangleq R_d - R_e$, and $a_2 \triangleq R_d + R_e$.

3 Qualitative Analysis of Vehicle Behaviors

3.1 Equilibrium formations

It is important to study vehicle behaviors under inter-vehicle interactions only. This is especially relevant after the vehicles enter the target area.

Proposition 3.1 *Let N be the number of vehicles. Then*

(1) the configuration of vehicles converges to some equilibrium;

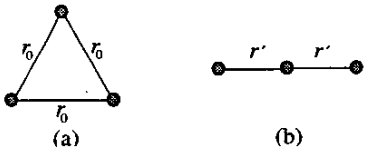

Fig. 1: Equilibrium configurations for $N = 3$.

(2) for $N = 2$, if $\|p_1(0) - p_2(0)\| < R_c$, the vehicles maintain a distance of r_0 in the equilibrium configuration and the equilibrium is globally asymptotically stable;

(3) for $N = 3$, if $\|p_i(0) - p_j(0)\| < R_c$, $1 \leq i, j \leq 3$, the vehicles either form an equilateral triangle (Fig. 1(a)), or form a line at the equilibrium. If $\frac{df_n}{dr}$ is strictly increasing on $(0, r_0]$, the collinear configuration is equally spaced with spacing r' (Fig. 1(b)), where $\frac{r_0}{2} < r' < r_0$ and $\frac{df_n}{dr}(r') = -\frac{df_n}{dr}(2r')$. Furthermore, if $\frac{df_n}{dr}$ is strictly increasing on $[r_0, 2r_0]$, such r' is unique. The collinear configuration is unstable, while the equilateral configuration is locally asymptotically stable.

Sketch of proof. Take the sum J of the neighbouring potentials as a candidate Lyapunov function. Claim (1) follows from LaSalle's Invariance Principle. Claims (2) and (3) can be proved by explicitly deriving the condition for $\frac{dJ}{dt} = 0$. □

We note that similar results for the cases $N = 2, 3$ also appeared in [8] where the second order dynamics and a quadratic potential were considered. For general $N > 3$, one can design the potential function properly so that certain configurations (or *formations*) become equilibria that are *locally* asymptotically stable (also refer to [3] for a discussion on designing stable flocking and schooling motions using "virtual leaders"). For instance, if we design the function f_n with $R_c = \sqrt{3}r_0$, then lattices of equilateral triangles with length r_0 are such equilibria. These equilibria are often desirable: for instance, in the scenario of this paper, the vehicles would provide good area coverage while maintaining optimal inter-vehicle distance. However, due to the existence of multiple locally asymptotically stable equilibria, one cannot guarantee the convergence to a particular desired configuration. Although the ambiguity (of the final formation) can be eliminated using the *structural* potential functions [7], the latter approach requires explicit specification of the communication topology. Such requirement, unfortunately, is not feasible in our scenario, where some of the vehicles might get destroyed during the mission.

Despite the ambiguity problem, extensive simulation appears to support that the final formation is usually well "organized" under the purely local interactions. Fig. 2 shows the final formation of 30 vehicles starting from a random initialization.

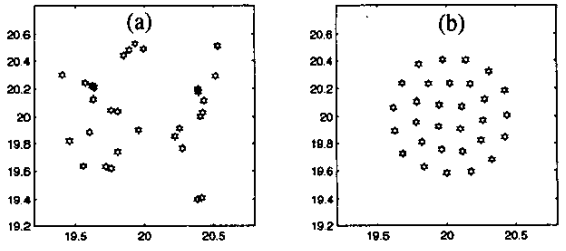

Fig. 2: Formation of 30 vehicles under local interactions: (a) random initialization; (b) final formation.

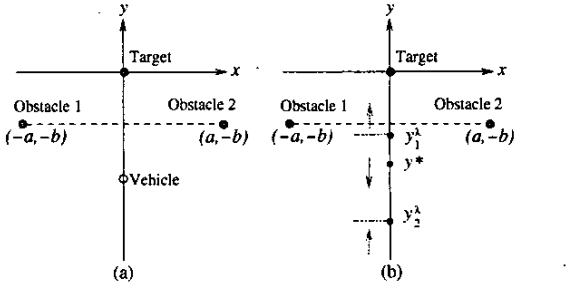

Fig. 3: (a) The setup of two obstacles and one target; (b) The vector field on the y axis.

3.2 Vector field analysis

Scenario I: In this sub-section we analyze the behavior of a vehicle when it experiences both the attraction from a target and the repulsion from obstacles. Two scenarios are considered. In the first one (illustrated in Fig. 3(a)), the (point) target is located at the origin (0,0), and two (point) obstacles are located symmetrically about the y axis with coordinates $(-a, -b)$ and $(a, -b)$, respectively $(a, b > 0)$. The potential function in terms of (x, y) is

$$\lambda(x^2 + y^2) + \frac{1}{(x+a)^2 + (y+b)^2} + \frac{1}{(x-a)^2 + (y+b)^2},$$

and the associated vector field is

$$\begin{cases} \dot{x}(t) = \frac{2(x+a)}{[(x+a)^2+(y+b)^2]^2} + \frac{2(x-a)}{[(x-a)^2+(y+b)^2]^2} - 2\lambda x \\ \dot{y}(t) = \frac{2(y+b)}{[(x+a)^2+(y+b)^2]^2} + \frac{2(y+b)}{[(x-a)^2+(y+b)^2]^2} - 2\lambda y \end{cases}, \tag{4}$$

where the weighting constant for obstacles equals 1. Consider a vehicle initially located on the y axis. We want to know whether it will move toward the target under the vector field (4) when $y < 0$ (the case $y > 0$ is simpler and can be studied similarly). Due to the symmetry, $\dot{x} = 0$, so the real question is whether $\dot{y} > 0$. When $x = 0$,

$$\dot{y} = \frac{4(y+b)}{[(a^2 + (y+b)^2]^2} - 2\lambda y. \tag{5}$$

Let $\tilde{y} = y + b$. Obviously, if $\tilde{y} \geq 0$, $\dot{y} > 0$. In the following we study the case $\tilde{y} < 0$.

Proposition 3.2 *There is a unique solution* $\tilde{y}^* \in (-\frac{a}{\sqrt{3}}, 0)$ *to*

$$4\tilde{y}^3 - 3b\tilde{y}^2 + a^2 b = 0. \tag{6}$$

Let

$$\lambda^* = \frac{2}{(a^2 + \tilde{y}^{*2})^2}(1 - \frac{4\tilde{y}^{*2}}{a^2 + \tilde{y}^{*2}}), \tag{7}$$

and $y^* = \tilde{y}^* - b$. *Then*

(1) If $\lambda > \lambda^*$, $\dot{y} > 0$, $\forall y < -b$;

(2) If $\lambda = \lambda^*$, $\dot{y} > 0$ *for* $y \in (-\infty, -b)$ *except at* y^* *where* $\dot{y} = 0$;

(3) If $\lambda < \lambda^*$, *there exist* y_1^λ, y_2^λ *dependent on* λ, $y_2^\lambda < y^* < y_1^\lambda$, *such that*

$$\begin{cases} \dot{y} > 0, \ \textit{if } y \in (-\infty, y_2^\lambda) \\ \dot{y} < 0, \ \textit{if } y \in (y_2^\lambda, y_1^\lambda) \\ \dot{y} > 0, \ \textit{if } y \in (y_1^\lambda, -b) \\ \dot{y} = 0, \ \textit{if } y = y_1^\lambda \ \textit{or} \ y_2^\lambda \end{cases},$$

as illustrated in Fig. 3(b). Furthermore, as λ *decreases from* λ^* *to 0,* y_1^λ *increases from* y^* *to* $-b$, *and* y_2^λ *decreases from* y^* *to* $-\infty$.

Proof. Let $h(\tilde{y}) = \frac{4\tilde{y}}{(a^2+\tilde{y}^2)^2}$. Since

$$\frac{dh}{d\tilde{y}} = \frac{4(a^2 - 3\tilde{y}^2)}{(a^2 + \tilde{y}^2)^2}, \tag{8}$$

$h(\tilde{y})$ is strictly decreasing on $(-\infty, -\frac{a}{\sqrt{3}})$, and strictly increasing on $(-\frac{a}{\sqrt{3}}, 0)$. From (8), $\frac{dh}{d\tilde{y}}$ is also strictly increasing on $(-\frac{a}{\sqrt{3}}, 0)$. Graphical analysis reveals that there exists a unique λ^*, such that the line $l(\tilde{y}) = 2\lambda^*(\tilde{y} - b)$ is tangent to the curve $h(\tilde{y})$ at a unique $\tilde{y}^* \in (-\frac{a}{\sqrt{3}}, 0)$. After algebraic manipulations, one can show that $\tilde{y}^*$ satisfies (6) and λ^* is defined by (7). The remaining claims of the proposition follow from the graphical analysis. □

From Proposition 3.2, the weight λ determines whether the vehicle can pass the obstacle potential valley and get to the target.

Scenario II: Next we investigate the motion of a vehicle in the presence of one point target (0,0) and one point obstacle $(0, -b)$. Here no constraint on the vehicle position is imposed except that we focus on the region $y < 0$ (the case $y > 0$ is simpler and can be analyzed similarly). The vector field is

$$\begin{cases} \dot{x} = \frac{2x}{[x^2+(y+b)^2]^2} - 2\lambda x \\ \dot{y} = \frac{2(y+b)}{[x^2+(y+b)^2]^2} - 2\lambda y \end{cases}. \tag{9}$$

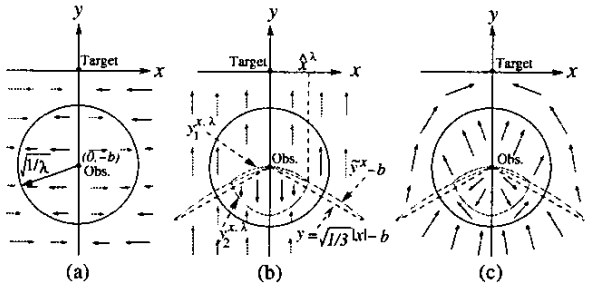

Fig. 4: Vector field analysis for the case of one obstacle and one target. (a) x-component; (b) y-component; (c) total vector field.

We will discuss $\dot{x}$ and $\dot{y}$ separately. Denote by $\mathcal{C}_\lambda$ the circle with radius $\frac{1}{\sqrt{\lambda}}$ centered at $(0, -b)$, $\mathcal{C}_\lambda^-$ the region inside $\mathcal{C}_\lambda$, and $\mathcal{C}_\lambda^+$ the region outside $\mathcal{C}_\lambda$. Then clearly

$$\begin{cases} \dot{x} > 0, \text{ if } x < 0, (x,y) \in \mathcal{C}_\lambda^+ \text{ or } x > 0, (x,y) \in \mathcal{C}_\lambda^- \\ \dot{x} < 0, \text{ if } x > 0, (x,y) \in \mathcal{C}_\lambda^+ \text{ or } x < 0, (x,y) \in \mathcal{C}_\lambda^- \\ \dot{x} = 0, \text{ if } x = 0 \text{ or } (x,y) \in \mathcal{C}_\lambda \end{cases},$$

as shown in Fig. 4(a).

For $\dot{y}$, it's straightforward to verify

$$\dot{y} > 0 \text{ if } (x,y) \in \mathcal{C}_\lambda^+ \text{ or } y \geq -b.$$

However, the analysis is more involved when $y < -b$ and $(x,y) \in \mathcal{C}_\lambda^-$. The proof of the following result can be found in [10], and it shares the spirit of the proof for Proposition 3.2:

Proposition 3.3 *Let* $\tilde{y} = y + b$. *For each* x, *there exists a unique* $\tilde{y}^x \in (-\frac{\sqrt{3}}{3}|x|, 0)$ *satisfying*

$$4\tilde{y}^3 - 3b\tilde{y}^2 + bx^2 = 0,$$

$\tilde{y}^x = \tilde{y}^{-x}$, *and* $\tilde{y}^x$ *strictly decreases as* $|x|$ *increases. Let* $y^x = \tilde{y}^x - b$. *For* $\lambda > 0$, *there is an* $\hat{x}^\lambda > 0$ *with* $(\hat{x}^\lambda, y^{\hat{x}^\lambda}) \in \mathcal{C}_\lambda^-$, *and two continuous functions* $y_1^{x,\lambda}$ *and* $y_2^{x,\lambda}$ *of* x *defined on* $[0, \hat{x}^\lambda]$, *dependent on* λ, *that satisfy the following:*

(1) $y_1^{x,\lambda}$ *decreases as* $|x|$ *increases,* $y_1^{x,\lambda} = y_1^{-x,\lambda}$, $y_1^{x,\lambda} \geq y^x$ *where the equality holds only at* $x = 0$ *and* $x = \hat{x}^\lambda$;

(2) $y_2^{x,\lambda}$ *increases as* $|x|$ *increases,* $y_2^{x,\lambda} = y_2^{-x,\lambda}$, $y_2^{x,\lambda} \leq y^x$ *where the equality holds only at* $x = 0$ *and* $x = \hat{x}^\lambda$.

Denote the region enclosed by the graphs of $y_1^{x,\lambda}$ *and* $y_2^{x,\lambda}$ *as* $\mathcal{D}_\lambda$. *Then for the case* $y < 0$, $\dot{y} \leq 0$ *if and only if* $(x,y) \in \mathcal{D}_\lambda$, *where the equality holds only at the boundary of* $\mathcal{D}_\lambda$.

Fig. 4(b) illustrates Proposition 3.3 and sketches the y-component of the vector field. The total vector field

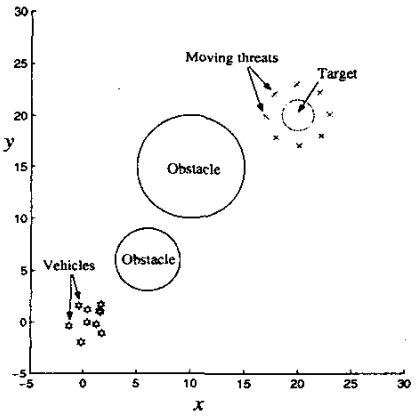

Fig. 5: The simulation scenario.

is shown in Fig. 4(c). The only point where $\dot{x} = \dot{y} = 0$ is $(0, y_2^{0,\lambda})$. But this is an unstable equilibrium as one can tell from the figure. We can also verify that the linearized system at $(0, y_2^{0,\lambda})$ has a positive eigenvalue. Hence for any $\lambda > 0$, the vehicle will not get blocked by the obstacle potential; but the larger λ, the less "detour" it takes before it moves towards the target.

4 Simulation Results

Fig. 5 shows the simulation scenario. There are ten vehicles (represented by the pentagons) randomly distributed in the left lower corner at $t = 0$. Two circular obstacles (with radii 3 and 5, respectively) sit between the vehicles and the target (also circular, with radius 1.5). Eight moving threats (represented by the crosses), uniformly distributed around the target, protect the target from invasion by the vehicles. Each threat moves with angular velocity 0.03 rad/sec and radius 3 (linear speed 0.09/sec), while each vehicle's maximum speed is 0.06/sec. There is no stationary threat in the field. The optimal inter-vehicle distance r_0 is 0.5, the communication range $R_c = \frac{\sqrt{3}}{2}$, the detection range R_d for moving threats is 3, and the killing range $R_e = 0.5$. If a vehicle is inside the target area, it's motion is not affected by the threats and the obstacles. To guarantee the vehicles are distributed around the target center after they successfully enter the target area, an additional attractive potential from the target center is also included. The simulation was conducted in Matlab, where the function "fmincon" was used to solve the constrained minimization problem for each vehicle.

Fig. 6 shows the effect of the weighting constant λ_m for the potential due to moving threats. Other weights are fixed for Fig. 6(a) through (d): $\lambda_g = 1000$, $\lambda_o = 200$, and $\lambda_n = 1000$. When $\lambda_m = 10$ (very small), the vehicles paid least attention to the threats and four of them were destroyed because of getting too close to the threats (Fig. 6(a)); when $\lambda_m = 50$, only one vehicle was destroyed while the others entered the target (Fig. 6(b)); when $\lambda_m = 200$, all vehicles entered the target successfully and in a timely manner (Fig. 6(c)); when $\lambda_m = 2000$, some vehicles were not able to enter the target because more attention was put on evasion from the threats (Fig. 6(d)). We note that in all cases, the vehicles inside the target area displayed certain formations.

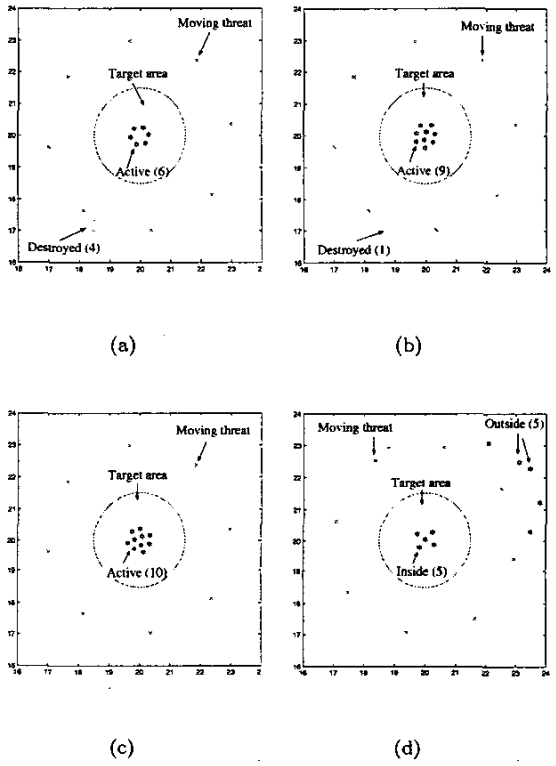

Fig. 6: Effects of the weighting coefficient λ_m for the moving threat potential. (a) $\lambda_m = 10$; (b) $\lambda_m = 50$; (c) $\lambda_m = 200$; (d) $\lambda_m = 2000$.

Fig. 7 demonstrates the effect of the weighting constant λ_o for the obstacle potential. Other weighting constants used are: $\lambda_g = 50$, $\lambda_n = 200$, $\lambda_m = 200$. When $\lambda_o = 1000$, one group of vehicles took the shorter path to pass the obstacle valley (Fig. 7(a)); but when $\lambda_o = 5000$, no vehicle took the shortcut (some actually took the detour), as shown in Fig. 7(b).

From the simulation results, we see that the decentralized approach based on potential functions lead to some emergent behaviors of vehicles. In addition, we can modify the behaviors by appropriately changing the weighting constants.

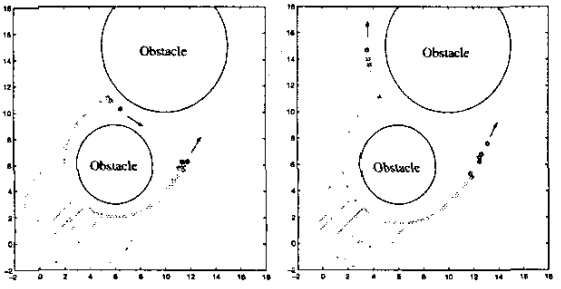

(a) (b)

Fig. 7: Effects of the weighting coefficient λ_o for the obstacle potential. (a) $\lambda_o = 1000$; (b) $\lambda_o = 5000$.

5 Conclusions

In this paper we have explored a decentralized approach to coordination and control of multi-vehicles using potential functions. A battlefield scenario was considered, in which the vehicles were required to occupy a target area (or point), avoid obstacles, evade threats, and maintain reasonable inter-vehicle distances. Stability of the equilibrium formations was briefly discussed. The behavior of a single vehicle was analyzed in the presence of an attractive target and (one or two) repulsive objects, and the effect of the weighting coefficient was studied. Simulation was conducted and interesting emergent behaviors were observed. We note that the analysis based on the vector field cannot be easily extended when two or more vehicles interact.

The most important advantage of this approach is its simplicity since only local or static information is needed in the path generation. It is also flexible and robust, which is of vital importance in complex, dynamic environments such as the battlefields. The drawback of the approach is that the possibility of being trapped in local minima exists. This has been a long time concern in the studies of the potential function method [11]. Practically interactions between vehicles and dynamic changes in the environment may prevent a vehicle from being trapped. Artificially introduced perturbation will also help to resolve this problem [12]. Another alternative is to incorporate other obstacle avoidance schemes based on, e.g, the contact dynamics models [13].

As shown in the simulation results, the choice of the weighting coefficients for different potential functions has a decisive impact on the vehicle behaviors and the mission outcome. Our future work will study how to design these weights in a systematic manner given the mission requirements.

References

[1] D. A. Schoenwald, "AUVs: in space, air, water, and on the ground," *IEEE Control Systems Magazine*, vol. 20, no. 6, pp. 15–18, Dec. 2000.

[2] K. M. Passino, "Biomimicry of bacterial foraging for distributed optimization and control," *IEEE Control Systems Magazine*, vol. 22, no. 3, pp. 52–67, 2002.

[3] N. E. Leonard and E. Fiorelli, "Virtual leaders, artificial potentials and coordinated control of groups," in *Proceedings of the 40th IEEE Conference on Decision and Control*, Orlando, FL, 2001, pp. 2968–2973.

[4] H. V. Parunak, M. Purcell, and R. O'Connel, "Digital pheromones for autonomous coordination of swarming UAV's," in *Proceedings of AIAA 1st Technical Conference and Workshop on Unmanned Aerospace Vehicles, Systems, and Operations*, 2002.

[5] A. Jadbabaie, J. Lin, and A. S. Morse, "Coordination of groups of mobile autonomous agents using nearest neighbor rules," *IEEE Transactions on Automatic Control*, vol. 48, no. 6, pp. 988–1001, 2003.

[6] H. G. Tanner, A. Jadbabaie, and G. J. Pappas, "Stable flocking of mobile agents, Part I: fixed topology," in *Proceedings of the 42nd IEEE Conference on Decision and Control*, Maui, Hawaii, 2003.

[7] R. Olfati-Saber and R. M. Murray, "Distributed cooperative control of multiple vehicle formations using structural potential functions," in *Proceedings of the 15th IFAC World Congress*, Barcelona, Spain, 2002.

[8] R. Bachmayer and N. E. Leonard, "Vehicle networks for gradient descent in a sampled environment," in *Proceedings of the 41st IEEE Conference on Decision and Control*, Las Vegas, NV, 2002, pp. 112–117.

[9] E. Rimon and D. E. Koditschek, "Exact robot navigation using artificial potential functions," *IEEE Transactions on Robotics and Automation*, vol. 8, no. 5, pp. 501–518, 1992.

[10] J. S. Baras, X. Tan, and P. Hovareshti, "Decentralized control of autonomous vehicles," Tech. Rep. 2003-14, Institute for Systems Research, University of Maryland, 2003.

[11] R. Volpe and P. Khosla, "Manipulator control with superquadric artificial potential functions: theory and experiments," *IEEE Transactions on Systems, Man, and Cybernetics*, vol. 20, no. 6, pp. 1423–1436, 1990.

[12] J. Barraquand, L. Kavraki, J. Latombe, T. Li, R. Motwani, and P. Raghavan, "A random sampling scheme for path planning," *International Journal of Robotics Research*, vol. 16, no. 6, pp. 759–774, 1997.

[13] R. Fierro, P. Song, A. Das, and V. Kumar, "Cooperative control of robot formations," in *Cooperative Control and Optimization*, R. Murphey and P. M. Pardalos, Eds. 2002, pp. 73–93, Kluwer Academic Publishers.